https://chemclassjournal.com/
ChemClass Journal Vol. 9 Issue 4 (2025); 76 - 91
e-ISSN:3092-8214 p-ISSN:3092-8206
doi.org/10.33003/chemclass-2025-0904/07

Optimization of High Surface Area Magnetic Biochar Production from Coconut (*Cocos nucifera L.*) Shell with $FeCl_3$ using Response Surface Methodology

Chima Maximus Ejimadu*, James Majebi Okuo, and Felix Ebhodaghe Okieimen

University of Benin, Department of Chemistry, Centre for Biomaterials Research, Benin City.

***Corresponding author:** Email: ejimaduchimadu@gmail.com Tel. No. +2348075872479.

Abstract

In this study coconut shell biochar obtained by slow pyrolysis at 450°C was subsequently co-pyrolysed with $FeCl_3$ to obtain Fe^{3+} - doped magnetic biochar. The effects of the co-pyrolysis process variables: heat treatment temperature, duration of heat treatment, metal loads on the specific (BET) surface area of the magnetic biochar produced was optimized using response surface methodology (RSM) with central composite design (CCD). The optimum BET surface area ($m^2.g^{-1}$) of 2106.42 predicted from the model at process condition of metal loading 3.01 wt%, heat treatment temperature 327.88°C and duration of heat treatment of 1.627 hr was about 3-fold higher than the value for the precursor biochar (712.00 $m^2.g^{-1}$). The BET surface area of the magnetic biochar sample prepared using the optimum process conditions predicted by the model (2098.04 $m^2.g^{-1}$) was found to be within 2% margin of the value obtained from the model; thus validating the model. The physicochemical properties, surface oxygen functional groups, surface morphology, and EDX surface elemental composition of the magnetic and unmodified biochar samples were determined. Improvement in physical chemical properties, surface morphology and textural properties in this reported for the Fe^{3+} - doped biochar in the study are relevant to its application as sorbent for organic and inorganic contaminants, for environmental remediation, agronomic benefits and as catalyst / catalyst support.

Keywords: Biochar; Magnetic biochar; Physicochemical properties; Textural properties; Optimization.

Introduction

Pyrolysis is an important aspect of the thermochemical technology that has received considerable attention in the conversion of biomass into materials with potential in diverse applications. For instance, biochar, the major product of slow pyrolysis of biomass has reportedly found multifunctional applications that include: soil application for agronomic benefits and environmental remediation including carbon sequestration [1-4]. The properties of biochar: physicochemical properties, surface chemistry and morphology, including textural properties, upon which the ultimate utility of biochar depends, can be modified/altered through chemical and physical process leading to the

© CSN Zaria Chapter

production of activated carbons. For instance Yahia et al. [5], Li et al. [6], Tsai et al. [7], Sari et al. [8], Adorma et al. [9] reported on the preparation of activated carbon, through physical and/or chemical methods, of several feedstocks including coconut shell and reported that activation improved the measured physicochemical and chemical properties of the carbons. However, application of activated carbon in waste water treatment for the removal of contaminants suffers from a major drawback: difficulty in the complete removal by filtration of the activated carbon, particularly powdered activated carbon, from the treated wastewater. In order to obviate their drawback, in addition with the need to explore and extend the areas of biochar application, have resulted to the development of magnetic biochar (carbon-rich materials) which can easily be separated from the treated wastewater by application of a magnet. Recent studies have shown that in addition to applications in environmental remediation [10-13], magnetic biochar has potential applications in data storage, electrochemical double layer capacitance, magnetic image etc. [14-16].

The most frequently used method for the preparation of magnetic biochar is the simultaneous pyrolysis of the biomass with the metal salt [17-18]. A two-stage pyrolytic method in which the biochar obtained from initial pyrolysis of biomass is followed by a second-step, co-pyrolysis of the biochar with metal salts to obtain magnetic biochar has been reported [19-20]. Although the two-stage pyrolysis method is more energy intensive, the co-pyrolysis step allows better incorporation of metallic components on or within the biochar structures, and could lead to enhanced properties, porosity, surface area etc. which are pertinent in many biochar applications [21].

In this paper, the optimization of the process variables, using response surface methodology (RSM) in the co-pyrolysis step of the preparation of Fe^{3+} -based coconut shell magnetic biochar is reported. Coconut shell (and husks) are generated in large quantities from coconut industry. Regarded as waste materials, coconut shell (and husks) are more often disposed by open-air burning or dumbed into the environment, both methods with considerable public health and environmental concerns. Pyrolytic conversion of coconut shell biomass to activated carbon has been reported [22-25]. The application of RSM for the optimization of the process variables for the preparation of activated carbon from coconut shell was reported by Anuwar et al. [26]. Process optimization using RSM in the preparation of Fe - doped (magnetic) biochar using the wet co-precipitation method using coconut shell was reported by Musa et al. [27]. There are no previous reports to the knowledge of the authors on the optimization, using RSM, of the process variables in the co-pyrolysis step in the preparation of magnetic biochar from coconut shell.

Materials and Methods

Coconut shells were obtained from a local market in Benin City, rinsed thoroughly with deionised water, dried at 80° C for 8 hr and then ground to 2mm size. The chemicals used in this study were of analytical grade and were used without further purification.

Methods

The two-stage method adopted for the preparation of magnetic biochar followed the procedure described by Tomin and Yadzani [19]: an initial stage of pyrolysis of the biomass followed by a co-pyrolysis step of the biochar obtained with the metal salt.

Pyrolysis of coconut shell: Slow pyrolysis of coconut shell at various heat treatment temperatures, 350 - 700°C at a heating rate of 10^{o} min^{-1}, and the duration of heat treatment at maximum heat treatment temperature of 30 min under limited oxygen atmosphere, produced biochar samples which were subjected to textural analysis to obtain the biochar sample with optimal specific (BET) surface area. The biochar sample prepared at 450° C gave the optimal BET surface area [28] and was used in the second stage, co-pyrolysis with $FeCl_3$.

Preparation of Fe^{3+} - based magnetic biochar

A known amount of the biochar with optimal BET surface area was slurred in an aqueous solution of known amount of $FeCl_3$ salt. The slurry obtained was air-dried and then dried in an oven at 80° c for 3 hr. The dry material was there after co-pyrolysed to obtain magnetic biochar.

A statistical approach, response surface methodology (RSM) (Design Expert 11, Stat-ease, Inc., Minneapolis, USA) was adopted to optimize the second stage co-pyrolysis step for the preparation of magnetic biochar samples. RSM combines mathematical and statistical tools to optimize the effect of multiple process variables on the properties of the prepared products [29,30]

Central composite design (CCD) a key aspect of RSM, was used to study the effect of the co-pyrolysis process; metal loading, heat treatment temperature and duration of heat treatment on this BET surface area of the magnetic biochar. Table 1 gives the range and levels of the independent variables used in the preparation of the magnetic biochar samples. Nineteen experiments were suggested by the design of experiment for magnetic carbon-rich material production. The response for each run, specific (BET) surface area was then statistically analyzed by a software to obtain the optimum conditions, the interaction between the process variables and the factor(s) that optimize the process [31].

Table 1: CCD experimental conditions for the Fe metal doping of biochar process

Independent variables	Coding	Level		
		-1	0	+1
Fe loading (wt%)	A	0.558	3.071	5.584
Temperature (°C)	B	250	375	500
Time (hr)	C	1	2.5	4

Results and Discussion

The results of the experimental runs used in the determination of BET surface area of the magnetic Fe^{3+} - based carbon-rich materials from the central composite design (CCD) are given in Table 2.

Table 2: Experimental runs for BET surface area determination of Fe^{3+} - based biochar

S/N	Fe^{3+} loading (wt % BC)	Temperature (° C)	Time (hr)	Surface area ($m^2.g^{-1}$)	
				Actual	Predicted
1	1.58	301	1.6	1897.21	1775.00
2	4.57	301	1.6	1794.53	1794.96
3	1.58	449	1.6	1186.10	1183.22
4	4.57	449	1.6	705.65	634.22
5	1.58	301	3.4	1185.18	1233.65
6	4.57	301	3.4	986.37	966.29
7	1.58	449	3.4	1859.24	1835.85
8	4.57	449	3.4	900.28	999.53
9	0.56	375	2.5	1270.46	1318.86
10	5.58	375	2.5	648.31	632.39
11	3.07	250	2.5	1403.22	1447.69
12	3.07	500	2.5	990.00	978.01
13	3.07	375	1.0	1794.64	1900.17
14	3.07	375	4.0	1825.18	1752.13
15	3.07	375	2.5	1993.22	1921.31
16	3.07	375	2.5	1879.36	1921.31
17	3.07	375	2.5	1878.33	1921.31
18	3.07	375	2.5	1871.02	1921.31
19	3.07	375	2.5	1990.18	1921.31

Table 2 gives the results of the experimental runs used to determine the response, BET surface area, of the magnetic Fe^{3+} - based biochar. It is apparent from the results that maximum value of BET surface area (1993.20 $m^2.g^{-1}$) was attained at a maximum heat treatment temperature of 375° C, at a duration of heat treatment temperature at maximum heat treatment temperature of 3 hr and using Fe^{3+} - loading of 3.07 wt%. The correlation

between the predicted and actual values of the specific area is shown in Fig. 1.

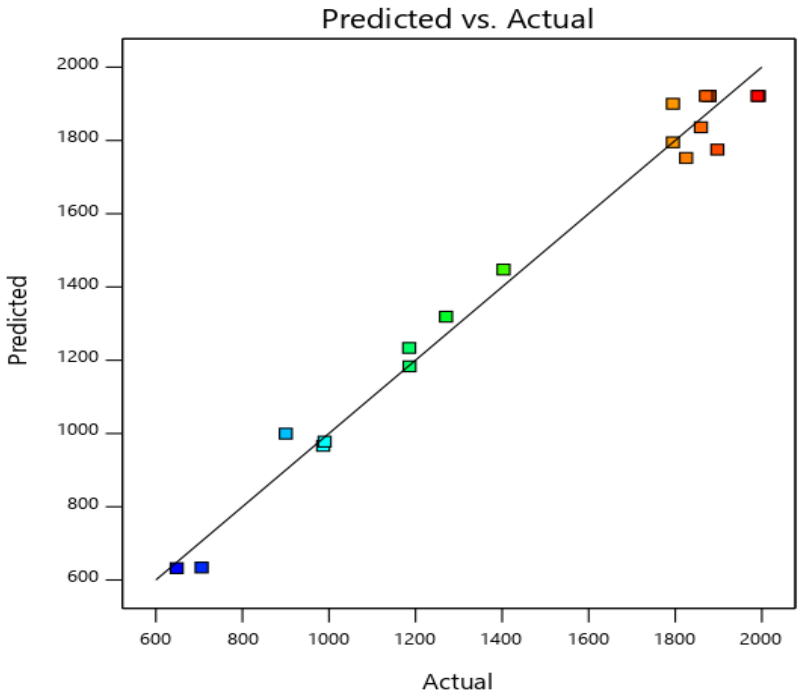


Fig 1: Correlation between the actual and predicted value of Fe^{3+} - based biochar

The close correlation of the predicted and actual values of this BET surface area is by the high R^2 value; predicted 0.8822 and adjusted 0.9645 from the quadratic model equation, that was suggest as a better fit for the evolution of BET surface area in Fe^{3+} - based coconut shell biochar (Table 3).

Table 3: Summary of model statistic of BET surface area of Fe^{3+} - based biochar

Source	Sequential p-value	Lack of Fit p-value	Adjusted R^2	Predicted R^2	
Linear	0.2847	0.0005	0.0608	-0.2659	
2FI	0.2248	0.0005	0.1727	-0.2069	
Quadratic	**< 0.0001**	**0.1776**	**0.9645**	**0.8822**	**Suggested**
Cubic	0.1029	0.4624	0.9830	0.8466	Aliased

Analysis of variance(ANOVA) was used in fitting the quadratic response surface model by the least square method and to test the extent of suitability of the model at a confident level of 95% (5% significant level). The ANOVA results Table 4, indicate that the variables, A, B, C, AB, AC, BC, A^2, B^2 were significant and the F regression of value of 55.27 indicate that the

model was significant and validated by the p-value less than 0.0001.

Table 4: Anova of BET surface area of Fe^{3+} - based biochar

Source	Sum of Squares	df	Mean Square	F-value	P-value	
Model	3.893E+06	9	4.326E+05	55.27	< 0.0001	**Significant**
A-Conc.	5.688E+05	1	5.688E+05	72.68	< 0.0001	
B-Temp.	2.663E+05	1	2.663E+05	34.02	0.0002	
C-Time	26453.44	1	26453.44	3.38	0.0991	
AB	1.619E+05	1	1.619E+05	20.68	0.0014	
AC	41276.39	1	41276.39	5.27	0.0473	
BC	7.128E+05	1	7.128E+05	91.08	< 0.0001	
A^2	1.526E+06	1	1.526E+06	194.98	< 0.0001	
B^2	8.564E+05	1	8.564E+05	109.43	< 0.0001	
C^2	15450.40	1	15450.40	1.97	0.1936	
Residual	70435.64	9	7826.18			
Lack of Fit	54391.53	5	10878.31	2.71	0.1776	**not significant**
Pure Error	16044.11	4	4011.03			
Cor Total	3.964E+06	18				

The main linear factors: metal loading (A), and maximum heat treatment temperature (B) had p-values less than 0.05 and are considered significant variables affecting the evolution of specific surface in the co-pyrolysis step, while duration of heat treatment at maximum heat treatment temperature (C) with p-value greater than 0.05 was deemed insignificant. Among the main linear factors, metal loading exhibited the strongest influence on the specific surface area, as indicated by its highest F-value (72.68). The interaction factors, AB, AC and BC were found to be significant, with the strongest being the interaction between the maximum heat treatment temperature and duration of heat treatment (BC, F-value 91.08), followed by the interaction between metal loading and maximum heat treatment temperature (AB) (F-value, 20.68), suggesting that the combined effects of these factors play a crucial role in determining the structural and textural properties of the biochar. All the quadratic factors A^2, B^2 except C^2 gave p-values lower than 0.05 and are considered significant factors. The quadratic effect of metal loading (A^2) (F-value, 194.98) contributed strongest in affecting BET surface area developed in the co-pyrolysis step of magnetic biochar preparation. The evolved quadratic equation for the optimization of process variables leading to the preparation of magnetic Fe^{3+} - based biochar is giving in Egn. 1.

For Fe^{3+}- based magnetic biochar

BET Surface area = +1921.31 -204.09A -139.63B -44.01C -142.24AB -71.83AC +298.50BC $-334.35A^2$ $-250.48B^2$ $-33.64C^2$ (1)

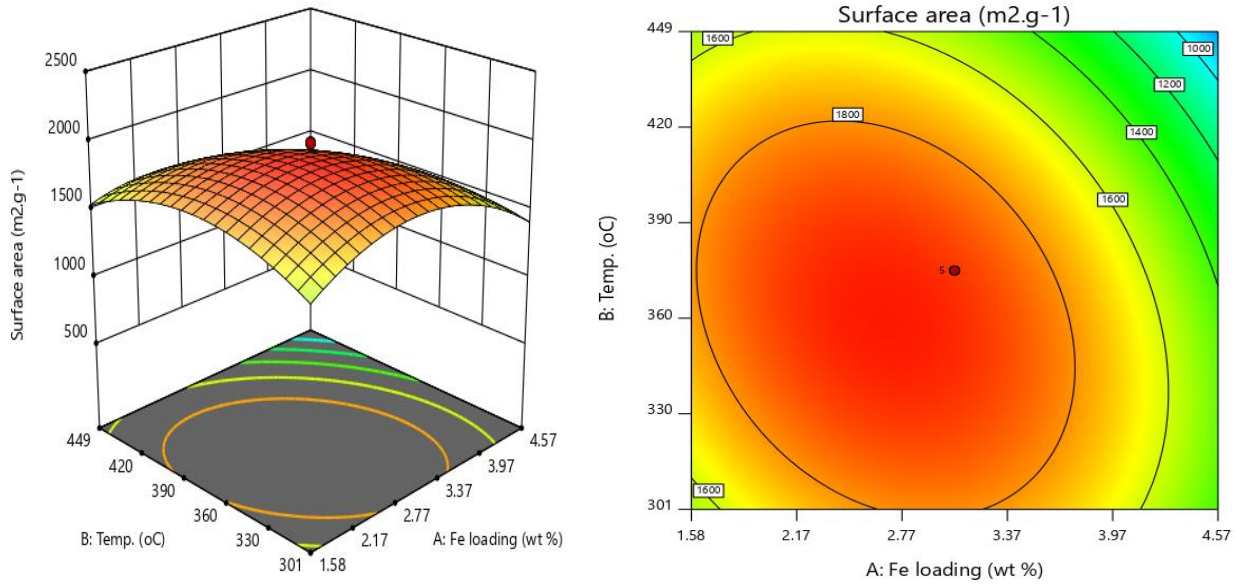
It can be seen from Egn.1 that the main, interaction (except the interaction between temperature of maximum heat treatment (B) and duration of heat treatment at maximum heat treatment temperature (C), i.e BC) had negative effect on BET surface area development; i.e an increase in the variables, except, BC, is not a complaint accompanied with increase in BET surface area of the magnetic biochar.

The features of the model as described using the fit statistics (Table 5) shows a coefficient of variation (CV) of 5.99% for BET surface area of the magnetic biochar and is within the acceptable range 5.31 and 8.06 [32]. The value of 20.08 reported for adequate precision is higher than 4.0, the designated threshold value for adequate signal and indicate that the model can be used to navigate the design space.

Table 5: Fit Statistics for Fe^{3+} - Doped Biochar

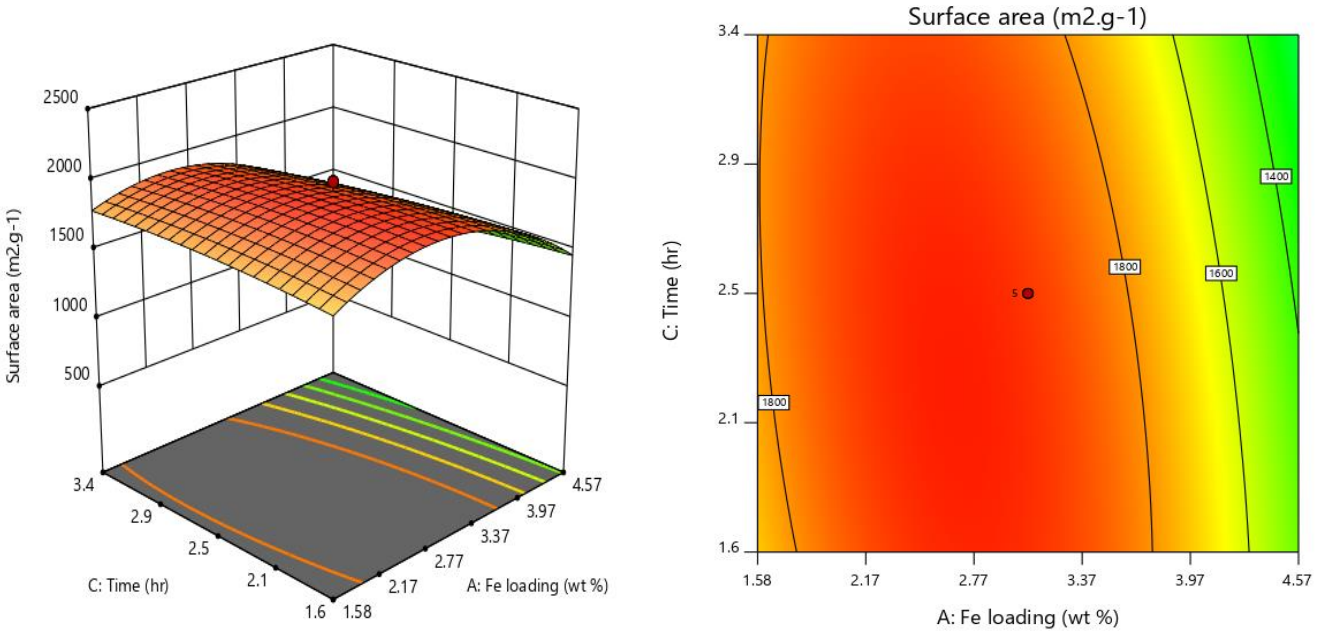
Parameter	Fe^{3+}-Based Biochar
Std. Dev.	88.47
Mean	1476.76
C.V. %	5.99
R^2	0.9822
Adjusted R^2	0.9645
Predicted R^2	0.8822
Adeq Precision	20.0830

Figure 2 shows the 3D response surface and contour plots of the effects of Fe^{3+} metal loading, maximum heat treatment temperature and duration of heat treatment at maximum heat treatment temperature on the BET surface area of magnetic biochar. It can be seen in Fig 2(a) that simultaneous increase in Fe^{3+} loading and maximum heat treatment temperature was accompanied with a decrease in BET surface area of the magnetic biochar. However, simultaneous increase in Fe^{3+} metal loading and duration of heat treatment at maximum heat treatment temperature resulted to higher values of BET surface area of the magnetic biochar (Fig. 2b).



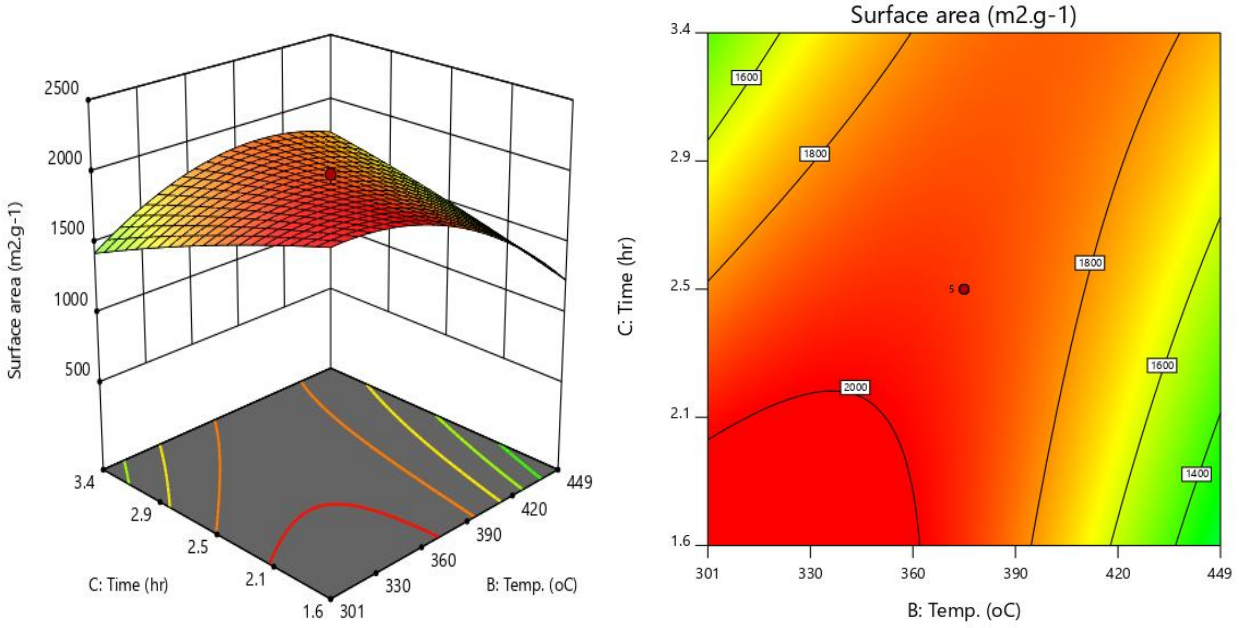
(a)

Fig. 2 (a): 3D and Contour Plots for Fe^{3+} - Loading and Heat Treatment Temperature on the BET Surface Area



(b)

Fig. 2 (b): 3D and Contour Plots for Fe^{3+} - Loading and Duration of Heat Treatment on the BET Surface Area



(c)

Fig. 2 (c): 3D and Contour Plots for Heat Treatment Temperature and Duration of Heat Treatment on the BET Surface Area

Increase in maximum heat treatment temperature and duration of heat treatment at maximum heat treatment temperature resulted to increase in BET surface area of the product magnetic biochar (Fig. 2c). The optimum BET surface area of magnetic coconut shell biochar obtaining response surface methodology using the two-stage pyrolysis method and the optimum process conditions are given in Table 6.

Table 6: Optimum BET surface area and optimum process variables for preparation of Fe^{3+} - based magnetic biochar

Parameters	Values
Fe^{3+} loading (wt %)	3.01
Maximum heat treatment temp. (°C)	327.877
Deviation of heat treatment (hr)	1.627
Optimum BET surface area ($m^2.g^{-1}$)	2106.421 (2098.04)
Desirability (%)	100

Values in parentheses are predicted from the model

Validation of the model

To validate the accuracy of the model, magnetic biochar sample was prepared using the optimum process conditions (and the procedure adopted for preparing the model samples.,) and the BET surface area determined, as described previously and given in parenthesis in Table 5. It can be seen that the values of BET surface area predicted by the model is well within 0.5% of the value determined for the sample prepared using the

optimum process conditions predicted by the model. This validates the model for projecting surface area evolution in Fe^{3+} - based magnetic coconut shell biochar.

Comparison of the physicochemical properties of coconut shell biochar and magnetic biochar.

Table 7 gives a comparison of the coconut shell biochar with optimal BET surface area [28] and magnetic biochar obtained therefrom at optimum co-pyrolysis process conditions.

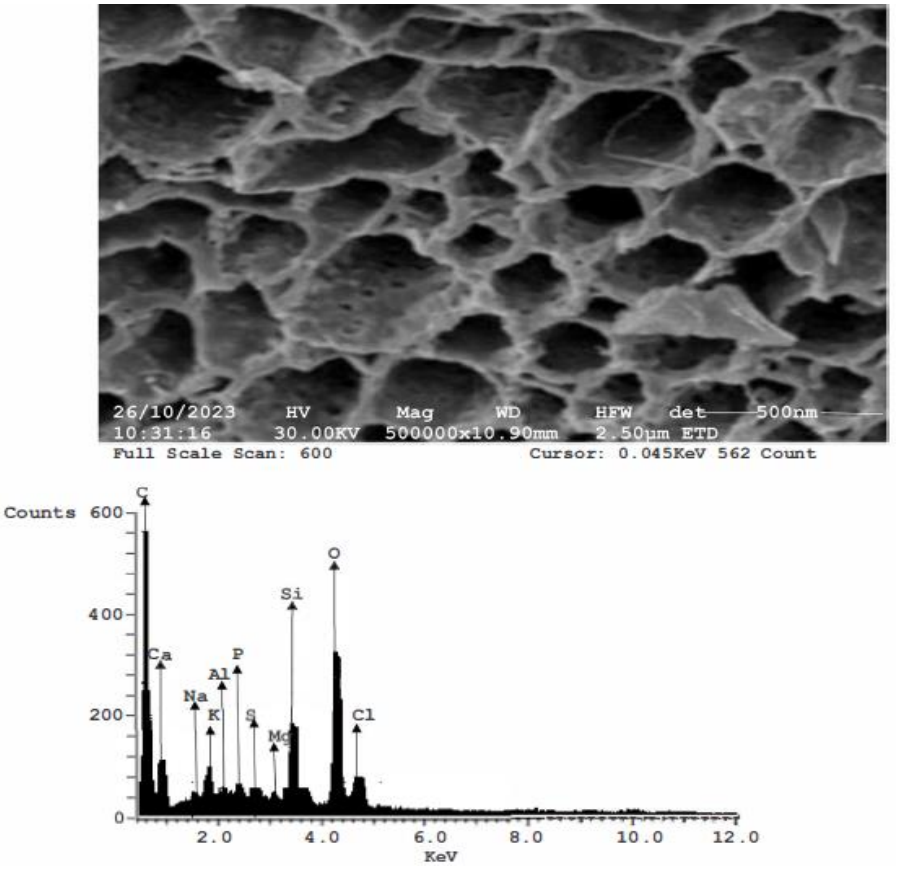
Table 7: Comparison of the Coconut Shell Biochar and Magnetic Biochar

Properties	**Biochar materials**	
	CSB450	**Fe^{3+} - based biochar MCSB**
Physicochemical Properties		
Ph	9.73 ± 1.11	5.43 ± 1.11
Bulk density (g.cm-3)	0.91 ± 0.18	0.94 ± 0.22
Electrical conductivity (**ms.cm^{-1}**)	12.18 ± 1.07	37.34 ± 1.15
Cation exchange capacity (cmol.kg-1)	28.03 ± 2.00	35.33 ± 0.84
Total surface oxygen functional groups (%)	3.47	2.17
Textural Properties		
S_{BET} ($m^2.g^{-1}$)	712.00	2098.04
Pore diameter (nm)	2.11	2.34
Pore volume ($cm^3.g^{-1}$)	0.36	0.91

CSB450 = coconut shell biochar at pyrolysis temperature of 450ºC
MCSB = magnetic coconut shell biochar obtained using optimum co-pyrolysis process conditions from RSM modelling

It can be seen from the results in Table 6 that the pH of the biochar sample was higher, by about 3 pH units than that of the magnetic biochar, while the total surface oxygen functional groups on the magnetic biochar was about 1.30% lower than for the biochar. The values of the physicochemical properties that are pertinent to soil application of biochar for bulk density, cation exchange capacity and electrical conductivity, were markedly higher for the magnetic biochar than for the biochar and are similar to the trend reported by Musa et al. [33] and Ogede et al. [34]. The overall improvements in the properties of the magnetic biochar are relevant to its soil application for agronomic and environmental benefits.

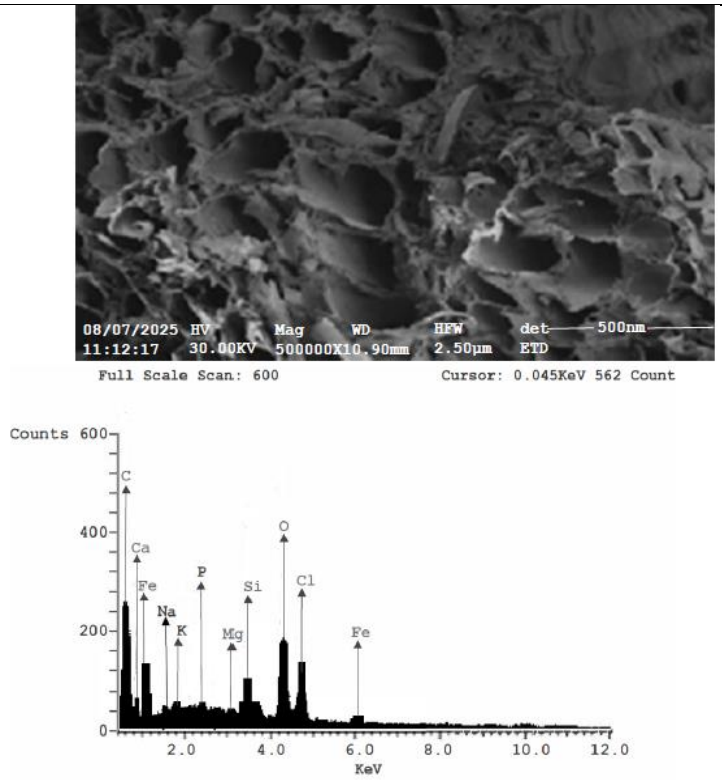
The scanning electron micrographs and surface elemental composition determined by energy dispersive X-ray (SEM/EDX) of the biochar and magnetic biochar samples are shown in Fig. 3.



(a)

Elements	Composition (%)
C	66.03
O	18.40
Ca	2.02
Si	3.92
Al	0.91
K	2.11
Na	1.55
Mg	1.50
P	1.34
Cl	2.09
S	0.12

Elements	Composition (%)
C	58.11
O	13.61
Ca	1.36
Si	3.11
K	1.18
Na	1.15
Mg	1.23
P	0.52
Cl	9.63
Fe	10.09



(b)

Fig. 3: SEM/EDX of (a) biochar (CSB450) and (b) magnetic biochar (MCSB) from coconut shell

It can be seen from the SEM micrographs that both biochar and magnetic biochar have porous (mesoporous; pore diameter less than 3nm). The more dominant elements on the surface of the materials were C 66% and 58%, O 18.40% and 13.61%, in the biochar and magnetic biochar samples respectively with O:C ratios of 0.278 and 0.231 respectively. The level of Fe^{3+} incorporated on the surface of the biochar was 10.09% . The textural properties; specific surface area, pore diameter and pore volume can be seen to be generally higher for the Fe^{3+} - doped biochar than the precursor biochar. The observed improvements in the textural properties of the Fe^{3+} -doped biochar can be explained in terms of synergetic processes; i) simultaneous lowering of the decomposition temperature of the biomass decarboxylation and/ decarbonylation reactions leading to the formation of microporous structures [35], ii) Carbon gasification reactions catalysed by Fe^{3+}/Fe^{2+} , and the associated removal of volatiles and creation of micro cavities [36], iii) $FeCl_3$ as precursor of iron oxides acted as template – like agent, facilitating formation of mesopores [35] occurring during co-pyrolysis of $FeCl_3$ with the biochar.

Conclusion

Process development by response surface methodology was adopted in this study for the

optimization of the process variables; metal loading, heat treatment temperature and duration of heat treatment in the co-pyrolysis step leading to the preparation of Fe^{3+} - based magnetic biochar. The optimum process conditions of metal loading 3.01 wt%; heat treatment temperature 327.88° C and duration of heat treatment 1.62 hr were found to yield the optimum BET surface area of 216.42 $m^2.g^{-1}$. The model that predicted the optimum BET surface area was validated by the convergence (within 2%) of the values of BET surface area of the magnetic biochar prepared using the optimum process conditions and that was obtained from the model. The physicochemical properties, textural properties, surface oxygen functional groups, surface morphology and surface elemental compositions of the magnetic biochar showed remarkable improvement in comparison with the unmodified biochar. The improvement in properties in the magnetic biochar should find use in soil improvement, wastewater treatment and catalyst applications. This study is part of an on – going studies on the pyrolytic conversion of biomass into carbon-rich materials for multifunctional applications. Studies on the application of the metal – doped coconut shell as catalyst in Friedel – Craft alkylation is on – going and will be reported in future communication.

Reference

[1] Wang, J., Li, Z., Li, Y., Wang, Z., Liu, X., Liu, Z. and Ma, J. (2024). Evolution and correlation of the physiochemical properties of bamboo char under successive pyrolysis process. *Biochar,* 6:33. https://doi.org/10.1007/s42773-024-00321-6.

[2] Pradhan, S., Abdelaal, A. H., Mroue, K., Al-Ansari, T., Mackey, H. R., & McKay, G. (2020). Biochar from vegetable wastes: agro-environmental characterization. *Biochar,* 2:439–453. https://doi.org/10.1007/s42773-020-00069-9.

[3] Chang, J., Zhang, H., Cheng, H., Yan, Y., Chang, M., Cao, Y., … Yan, M. (2019). Spent *Ganoderma lucidum* substrate derived biochar as a new bio-adsorbent for Pb2+/Cd2+ removal in water. *Chemosphere, 125121.* doi:10.1016/j.chemosphere.2019.125121

[4] Obonukut, M., Alabi, S. and Jock, A. (2022). Biochar from cassava waste: A paradigm shift from waste to wealth. *In: Biochar - Productive Technologies, Properties and Applications.* DOI: 10.5772/intechopen.105965

[5] Yahia, E.H., Serafin, J., Román-Martínez, M.C., Sreńscek-Nazzal, J., Dziejarski, B., Saidi, M. and Ouzzine, M. (2025). Preparation of activated carbon from Moroccan argan press cake using KOH activation and its application for CO_2 adsorption. *Fuel*, 393:134922. https://doi.org/10.1016/j.fuel.2025.134922

[6] Li, Y., Yan, X., Cui, Z., Yuan, J., Xu, B., and Guidong, Y. (2024). Design and preparation of activated carbon with high specific surface area and porosity through an organic activator coupled with CO_2 activation. *Advanced Materials Interfaces*, 12(3). https://doi.org/10.1002/admi.202400450

[7] Tsai, C.-H., and Tsai, W.-T. (2023). Optimization of Physical Activation Process by CO_2 for Activated Carbon Preparation from Honduras Mahogany Pod

Husk. *Materials*, *16*(19):6558. https://doi.org/10.3390/ma16196558

[8] Sari, R.M., Gea, S., Wirjosentono, B., Hendrana, S. and Hutapea, Y.A. (2020). Improving quality and yield production of coconut shell charcoal through a modified pyrolysis reactor with tar scrubber to reduce smoke pollution. *Polish Journal of Environmental Studies*, 29(2):1815–1824. https://doi.org/10.15244/pjoes/110582

[9] Adorna, J. Jr., Borines, M., Dang, V.D., and Doong, R.-A. (2020). Coconut shell derived activated biochar–manganese dioxide nanocomposites for high performance capacitive deionization. *Desalination*, 492:114602. doi:10.1016/j.desal.2020.114602.

[10] Ke, W., Liu, Z., Zhu, F., Xie, Y., Hartley, W., Li, X., Wu, H. and Xue, S. (2023). Remediation potential of magnetic biochar in lead smelting sites: Insight from the complexation of dissolved organic matter with potentially toxic elements. *Journal of Environmental Management*, 344:118556. https://doi.org/10.1016/j.jenvman.2023.118556

[11] Kizito, S., Wu, S., Kipkemoi Kirui, W., Lei, M., Lu, Q., Bah, H., & Dong, R. (2015). Evaluation of slow pyrolyzed wood and rice husks biochar for adsorption of ammonium nitrogen from piggery manure anaerobic digestate slurry. Science of The Total Environment, 505:102-112.

[12] Naisse, C., Girardin, C., Lefevre, R., Pozzi, A., Maas, R., Stark, A., & Rumpel, C. (2014). Effect of physical weathering on the carbon sequestration potential of biochars and hydrochars in soil. GCB Bioenergy, 7(3), 488–496. doi:10.1111/gcbb.12158

[13] Crombie, K., Mašek, O., Sohi, S. P., Brownsort, P., & Cross, A. (2013). The effect of pyrolysis conditions on biochar stability as determined by three methods. GCB Bioenergy, 5(2):122–131. doi:10.1111/gcbb.12030

[14] Gong, R., Li, H., Liu, Y., Fu, J., Yi, J. and Feng, D. (2025). Preparation of novel multifunctional magnetic biochar integrating adsorption and degradation and application in printing and dyeing wastewater. *Journal of Contaminant Hydrology*, 274:104652. https://doi.org/10.1016/j.jconhyd.2025.104652

[15] Burke, A. (2007). R&D considerations for the performance and application of electrochemical capacitors. *Electrochimica Acta*, 53(3):1083–1091.

[16] Rufford, T.E., Hulicova-Jurcakova, D., Zhu, Z. and Lu, G-Q. (2010). A comparative study of chemical treatment by $FeCl_3$, $MgCl_2$, and $ZnCl_2$ on microstructure, surface chemistry, and double-layer capacitance of carbons from waste biomass. *Journal of Materials Research* 25(8):1451–1459

[17] Reddy, D.H.K. and Lee, S.M. (2014). Magnetic biochar composite: Facile synthesis, characterization, and application for heavy metal removal. *Colloids and Surfaces A: Physicochemical and Engineering Aspects*, 454:96–103.

[18] Zhao, X., Liao, Z., Zhao, Q., Yang, M., Li, D., Zhang, K., Wang, X., Zhang, H. & Zheng, B. (2025). A low cost magnetic biochar manufactured solely from solid wastes by one-step pyrolysis for removal of tetracycline. Sci Rep 15:30035 https://doi.org/10.1038/s41598-025-14532-9

[19] Tomin, O., Yazdani, M.R. (2022). Production and characterization of porous magnetic biochar: before and after phosphate adsorption insights. *J Porous Mater* 29:849 – 859. https://doi.org/10.1007/s10934-022-01217-1.

[20] Hu, X., Xu, J., Wu, M., Xing, J., Bi, W., Wang, K., Ma, J. and Liu, X. (2017). Effects of biomass pre-pyrolysis and pyrolysis

temperature on magnetic biochar properties. *Journal of Analytical and Applied Pyrolysis*, http://dx.doi.org/10.1016/j.jaap.2017.08.006

[21] Chen, B., Chen, Z. and Lv, S. (2011). A novel magnetic biochar efficiently sorbs organic pollutants and phosphate. *Bioresource Technology*, 102(2), pp.716–723.

[22] Noor, N.M., Shariff, A., Abdullah, N., and Aziz, S. (2019). Temperature effect on biochar properties from slow pyrolysis of coconut flesh waste. *Malaysian Journal of Fundamental and Applied Sciences, 15(2):153–158.* doi:10.11113/mjfas.v15n2.1015.

[23] Saleem, J., Baig Moghal, Z.K., Pradhan, S. and McKay, G. (2024). High-performance activated carbon from coconut shells for dye removal: study of isotherm and thermodynamics. *RSC Advances, 14:33797–33808*. https://doi.org/10.1039/D4RA06287F

[24] Suman, S., & Gautam, S. (2017). Pyrolysis of coconut husk biomass: Analysis of its biochar properties. Energy Sources, Part A: Recovery, Utilization, and Environmental Effects, 39(8):761–767. doi:10.1080/15567036.2016.12632

[25] Prauchner, M. J., & Rodríguez-Reinoso, F. (2012). Chemical versus physical activation of coconut shell: A comparative study. *Microporous and Mesoporous Materials, 152:163–171.* doi:10.1016/j.micromeso.2011.11.040

[26] Anuwar, N.A. and Megat Khamaruddin, P.F. (2020). Optimization of chemical activation conditions for activated carbon from coconut shell using response surface methodology (RSM) and its ability to adsorb CO_2. *Proceedings of the Third International Conference on Separation Technology*. https://doi.org/10.2991/aer.k.201229.032

[27] Musa, A., Sani, B., Badiru, F., Aliyu, I. and Dandajeh, A. (2021). Characterisation of magnetised and non-magnetised coconut shell biochars. Niger. Res. J. Eng. Environ. Sci., 6(2): 483 - 494. https://doi.org/10.5281/zenodo.5805085.

[28] Ejimadu, M.C., Okuo, J.M., Okieimen. (2025). Evolution of functionalities and structure of biochar in pyrolysis of coconut shell at different temperatures. *Acta Chemica Malaysia, 9(2):122-130.*

[29] Reza, A., Chen, L. and Mao, X. (2024). Response surface methodology for process optimization in livestock wastewater treatment: *A review*. *Heliyon*, 10(9):e30326. https://doi.org/10.1016/j.heliyon.2024.e30326

[30] Alkharisi, M. K., & Dahish, H. A. (2025). The Application of Response Surface Methodology and Machine Learning for Predicting the Compressive Strength of Recycled Aggregate Concrete Containing Polypropylene Fibers and Supplementary Cementitious Materials. Sustainability, 17(7), 2913. https://doi.org/10.3390/su17072913.

[31] Tan, I.A.W., Ahmad, A.L., and Hameed, B.H. (2008). Optimization of preparation conditions for activated carbons from coconut husk using response surface methodology. *Chemical Engineering Journal*, 137(3):462–470. https://doi.org/10.1016/j.cej.2007.04.031

[32] Kalu, A.M., Edore, B.E., Madojemu, G.O., Ejimadu, C.M., Idode, V.O. and Okieimen, F.E. (2021). Total hydrocarbon degradation of crude oil contaminated soil using mixture of poultry manure and biochar: Optimization of amendment process variables. *International Journal of Research in Chemistry and Environment*, 11(1):1–8.

[33] Musa, A., Sani, B.S., Ibrahim, F.B. and Adamu, A.D. (2021) 'Characterisation of magnetised and non-magnetised coconut

shell biochars', *Nigerian Research Journal of Engineering and Environmental Sciences*, 6(2), pp. 483–494. p-ISSN: 2635-3342; e-ISSN: 2635-3350.

[34] Ogede, L.O., Ejimadu, C.M. and Okieimen, F.E. (2024) 'Chemical and textural properties of melon seed shell-derived biochar relevant to their application in the remediation of contaminated soil', *Nigerian Research Journal of Engineering and Environmental Sciences*, 9(2), pp. 681–688.

[35] Yang, J., Zhao, Y., Ma, S., Zhu, B., Zhang, C. (2016). Mercury removal by magnetic biochar derived from simultaneous activation and magnetization od sawdust. Environ. Sci. Technol. 50: 12040 – 12047. http://doi.org/10.1021/acs.est.6b03743

[36] Xu, Z., Zhou, Y., Sun, Z., Zhang, D., Huang, Y., Gu, S., and Chen, W (2019). Understanding reaction and pore – forming mechanism between waste cotton woven and FeCl3 during the synthesis of magnetic activated carbon. Chemosphere, 241: 125120 doi: http://doi.org/10.1016/j.chemosphere,2019.125120